J Mater Sci (2009) 44:3589–3599
DOI 10.1007/s10853-009-3486-8

Modeling of thermal barrier coating temperature due to transmissive radiative heating

Geunsik Lim · Aravinda Kar

Received: 13 January 2009 / Accepted: 10 April 2009 / Published online: 28 April 2009

Abstract Thermal barrier coatings are generally designed to possess very low thermal conductivity to reduce the conduction heat transfer from the coating surface to the metal turbine blade beneath the coating. In high-temperature power generation systems, however, a considerable amount of radiative heat is produced during the combustion of fuels. This radiative heat can propagate through the coating and heat up the metal blade, and thereby reduce the effectiveness of the coating in lowering the thermal load on the blade. Therefore, radiative properties are essential parameters to design radiative barrier coatings. This article presents a combined radiation and conduction heat transfer model for the steady-state temperature distribution in semitransparent yttria-stabilized zirconia (YSZ) coatings. The results of the model show a temperature reduction up to 45 K for YSZ of high reflectance (80%) compared to the YSZ of low reflectance (20%). The reflectivities of YSZ and metal blade affect the temperature distribution significantly. Additionally, the absorption and scattering coefficients of YSZ, the thickness of the coating, and the thermal conductivities of YSZ and metal blade affect the temperature distribution.

Introduction

The development of ceramic coatings to protect materials for high temperature use is critical for power generation where high thermal efficiency is required. Such coatings can provide a thermal barrier between metal components and hot combustion gases, allowing higher combustion temperatures for improved turbine performance without component degradation. Much of the research on thermal barrier materials has been driven by the desirability to reduce thermal conductivity and improve microstructural stability at high temperatures. Such efforts considered convection and thermal radiation of hot combustion gases and conduction in the ceramic coating layer as the dominant heat transfer mechanisms. So, there were considerable interests in developing thermal barrier coatings (TBCs) with lower thermal conductivity to improve the performance of gas turbine systems. Klemens and co-workers [1, 2] described some of the fundamental concepts of thermal conduction and how thermal conductivity may be reduced by altering the microstructure and composition. They considered phonon energy transfer by lattice waves due to anharmonic interactions, scattering of waves by lattice defects, and reflection of waves by grain boundaries and interfaces. The properties of TBCs that affect such interactions include the chemical composition, pore content and architecture, or other aspects of the topology of the coating (e.g., layering and grain size) and, therefore, these attributes are generally modified to lower the thermal conductivity of TBCs. Singh and Wolfe [3] studied the properties of a variety of coatings produced by electron beam-physical vapor deposition with various compositions under different deposition conditions. Trice et al. [4] investigated the effect of heat treatment on the phase stability and microstructure of yttria-stabilized zirconia (YSZ) coating using X-ray diffraction and transmission electron microscope and observed that the thermal conductivity decreases due to heat treatment.

When thermal radiation becomes significant at elevated temperatures, the temperature distributions in the coating

G. Lim · A. Kar (✉)
Laser-Advanced Materials Processing Laboratory, Department of Mechanical, Materials and Aerospace Engineering, College of Optics and Photonics, Center for Research and Education in Optics and Lasers (CREOL), University of Central Florida, Orlando, FL 32816-2700, USA
e-mail: akar@creol.ucf.edu

G. Lim
e-mail: glim@creol.ucf.edu

and metal blade are affected by both the absorption of incident thermal radiation and the conduction heat flux. So, various optical properties—such as refraction index, absorption index, and absorption coefficient—will affect the performance of TBCs in addition to the thermophysical and mechanical properties, such as the thermal conductivity, melting point, oxidation stability, and thermal stability. The spectral radiative properties of materials—such as the reflectivity, absorptivity, transmissivity, and emissivity—allow analyzing the radiative heating of TBCs and metal blades due to the combustion gases emitting energy over a broad spectral range. Thermal radiations of certain wavelengths may transmit without being absorbed in the coating and, in that case, the radiative energy will be deposited on the metal blade depending on its reflectivity. On the other hand, thermal radiations of another spectral region may be absorbed in the coating and, in that case, the radiation acts as an internal heat source for the coating. These radiative effects should be considered to determine the temperature distribution in turbine blades for high-temperature applications. YSZ coatings, which are widely used as TBCs, are translucent over the thermal radiation spectral range [5].

As pointed out by Eldridge et al. [5], the infrared transmittance and reflectance of TBCs have important implications on the performance of these coatings as radiation barriers as well as affecting the measurements of the TBC thermal conductivity. To optimize the operating temperature of coatings, an accurate analysis of the temperature distribution is necessary to understand how any change in the combustion environment affects the temperatures of the coating and metal blade. According to Singh and co-workers [3, 6], increasing the reflectance by means of nano-layered coatings may decrease the surface temperature of gas turbine blades up to 180 °C, which could lead to a significant (more than 10 times) improvement in the blade lifetime. They also measured the reduction in the metal blade temperature because of multilayered reflective coatings.

Combined radiation and conduction energy transfers have been analyzed in several studies. Wang et al. [7] presented a two-flux model to account for the radiative and conductive heat fluxes, calculated the temperature distributions in the coating layer and the metal blade, and showed that multilayered coatings can reduce the metal surface temperature. Since the refractive index has significant influences on the radiative transfer in medium, they also analyzed the effects of complex refractive index on the radiative heat transfer in a single layer of semitransparent medium and in multilayered coatings because the real and imaginary parts of the complex refractive index affect the reflectivity while the imaginary part affect the absorption coefficient. Their simulation results showed that more than 50% reflectivity can be achieved in the wavelength range 0.45–5 μm for multilayered TBCs that are based solely on ceramics.

Siegel and Spuckler [8] modeled the effect of thermal radiation on the temperature distribution of TBCs in turbine engines for aerospace applications. They examined the effects of the photon scattering within the coating and the reflectivity of the coating, and reported that the scattering coefficient of YSZ coating is much larger than its absorption coefficient at wavelengths up to 5 μm. They examined that the largest increases in metal temperature is due to a high index of refraction of translucent coating. Absorption is the means of direct interaction of radiation with the energy equation, and the local radiant emission from the volume element also depends on the absorption coefficient. Another important radiative property is the coating refractive index; this is because internal radiant emission depends on the refractive index squared. A larger refractive index also increases external and internal reflections which lead to trapping of radiation within the material by multiple internal reflections.

Modelings for coupled conductive and radiative heat transfers in the presence of absorbing, emitting, and isotropic scattering media are also carried out by many investigators. Viskanta and Kim [9], Mahapatra et al. [10], and Spuckler and Siegel [11] proposed a steady-state model for coupled conduction–radiation heat transfer with semitransparent boundaries. Since the radiative heat flux depends strongly on temperature, accurate instantaneous temperature distributions were calculated based on a transient numerical model [12–14] with various radiative and thermal boundary conditions including internal reflections. The numerical method involved nodal analysis, Hottel's zonal method, and geometrical optics for ray tracing, and the solution allowed investigating the effects of optical thickness, conduction and radiation parameters, and the absorption coefficient on the coating temperature. The radiative and conductive properties of the coating need to be known accurately to calculate the temperature distribution correctly. Demange and Bejet [15] designed two methods for measuring the thermal properties of TBCs, such as the thermal diffusivity and specific heat capacity, and the radiative properties, such as the emissivity and absorption coefficient, of partially transparent ceramics. These properties are useful to understand the conductive and radiative heating phenomena within a semitransparent material and they allow predicting the temperature distribution in turbine blades exposed to radiation from a combustor.

This article presents a one-dimensional model for coupled conductive and radiative heat transfer in the TBC and metal blade at the steady state. The heating of the turbine blades by the hot combustion gases is considered to be due to two effects: convection heat transfer and radiative

heating. A convective boundary condition is applied at the free surface of the coating to account for the convection heat transfer. The heat transfer coefficient used in this boundary condition will also allow examining the effect of the coolant flowing out of the cooling holes at this coating surface. The radiation from the hot combustion gases is considered to undergo both scattering and absorption within the TBC layer. The absorption phenomenon is manifested as a volumetric heat source for radiative heating of the TBC layer. When the radiation propagates through the coating to incident on the metal blade, a fraction of the incident radiation is absorbed by the blade and the rest is reflected back toward the coating layer. The coating–bondcoat (BC) interface, in turn, allows a fraction of the reflected radiation to enter into the coating layer and the rest is reflected back onto the metal–BC interface. These back and forth reflections cause multiple reflections at the coating–BC and metal–BC interfaces, which are taken into account in this study. Also conjugate boundary conditions, i.e., the continuities of temperatures and heat fluxes, are considered at the metal–BC interface. To account for the effect of coolant flowing through the hollow space in the metal blade, a convection boundary condition is applied at the metal–coolant interface. The results of this article also indicate that a single coating layer of high reflectivity can be an effective RBC in contrast to the multilayered coatings discussed by Singh and Wolfe [3], Kelly et al. [6], and Wang et al. [7].

Mathematical model for radiative heating of TBC

Radiative and conductive heat transfers are analyzed in the TBC on superalloy turbine blades for evaluating the thermal protection characteristics of the coating in high-temperature turbine systems. The mathematical model becomes complicated when appreciable heat conduction occurs simultaneously with radiative heating in absorbing, emitting, and scattering media. Such models are generally solved using numerical methods to obtain the distributions of temperature and scattered energy, and the heat fluxes of interest. The analysis, however, is simplified greatly for one-dimensional heat transfer at the steady state, which is considered in this study. Since the coating thickness is much smaller than the coating surface area and the hot combustion gases flow turbulently around the turbine blades, the heat conduction can be considered one dimensional in the thickness direction. The curved surfaces of turbine blades and the blade size, i.e., the length of the blade being much larger than its width, make the heat transfer problem multidimensional. The one-dimensional heat transfer approximation, however, is expected to hold good over localized domains at various regions of the turbine blades.

Figure 1a shows the planar geometry of YSZ coating on a superalloy turbine blade with $x = 0$, L_Y, L_m, and L_c representing the free surface of the coating layer, and coating–BC, metal–BC, and coolant–metal interfaces, respectively. It illustrates the combined transport of thermal energy by conduction and radiation in the coating layer, which is considered semitransparent in this study. The hot combustion gases flow over the coating surface at $x = 0$ and thus cause convection heating of the surface with the heat transfer coefficient h_g. The thermal radiation from the combustion gases, on the other hand, enters into the coating layer and propagates toward the metal through the absorption and scattering mechanisms. To obtain an expression for the temperature distribution, $T_Y(x)$, in the YSZ coating layer, an elemental control volume of thickness Δx is considered as shown in Fig. 1b. The conservation of energy yields the following expression relating the conductive and radiative heat fluxes for this control volume at the steady state.

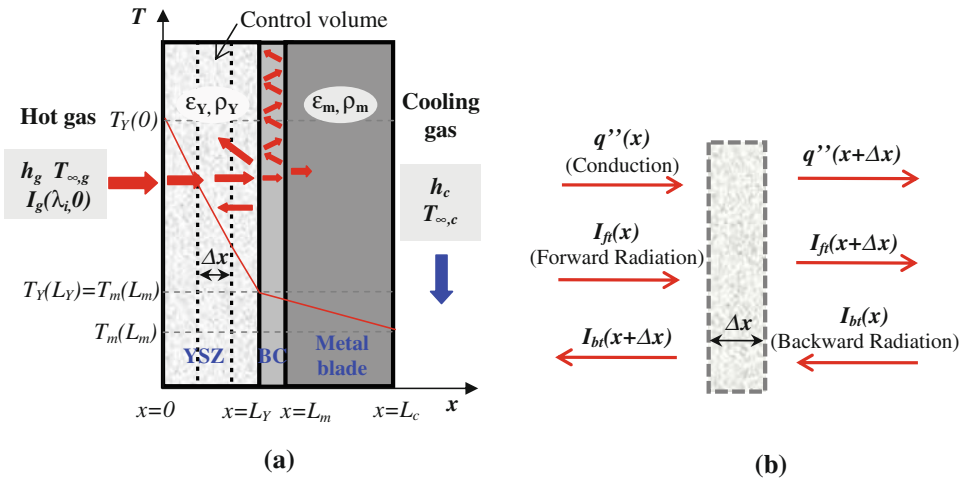

Fig. 1 **a** Geometrical representation of the turbine blade system for modeling conduction and radiative heating. **b** Typical control volume for energy balance

$$Aq''(x) + AI_{ft}(x) + AI_{bt}(x + \Delta x) - Aq''(x + \Delta x) - AI_{ft}(x + \Delta x) - AI_{bt}(x) = 0, \quad (1)$$

where A is the surface area normal to the direction of heat flow through the control volume in Fig. 1b and $q''(x)$ is the heat flux in the x direction in units of W/m^2. The heat transfer rate by conduction through the plane wall of area A is given by $q(x) = q''(x)A$. $I_{ft}(x)$ is the total intensity due to the forward-moving thermal radiations of different wavelengths emitted by the combustion gases. $I_{bt}(x)$ is the total intensity due to the backward-moving thermal radiations of different wavelengths. These backward-moving thermal radiations originate from the reflections at the metal–coating interface as shown in Fig. 2.

Dividing both sides of Eq. 1 by Δx, taking the limit as $\Delta x \to 0$ and utilizing the Fourier law of heat conduction, i.e., $q''(x) = -k_Y(T_Y)(dT_Y(x)/dx)$, where $k_Y(T_Y)$ is the temperature-dependent thermal conductivity of the YSZ coating, Eq. 1 can be written as follows for the temperature distribution in the coating layer.

$$\frac{d}{dx}\left[k_Y(T_Y)\frac{dT_Y(x)}{dx}\right] - \frac{dI_{ft}(x)}{dx} + \frac{dI_{bt}(x)}{dx} = 0. \quad (2)$$

Similarly, the governing equation for the temperature distribution in the metal blade is given by

$$\frac{d}{dx}\left[k_m(T_m)\frac{dT_m(x)}{dx}\right] = 0, \quad (3)$$

where $k_m(T_m)$ is the temperature-dependent thermal conductivity of the metal blade. Equations 2 and 3 are solved for $T_Y(x)$ and $T_m(x)$ under appropriate boundary conditions. Equation 2, however, involves the total radiative intensities of the thermal radiation, which can be determined as follows.

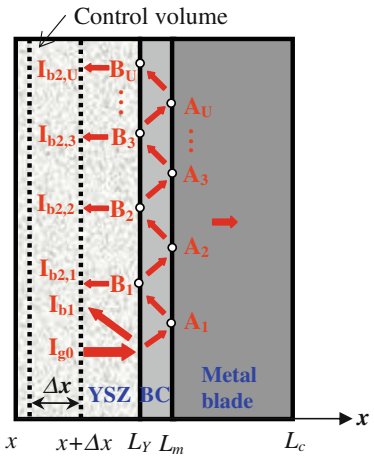

Fig. 2 Propagation of thermal radiation in various parts of the turbine blade system and multiple reflections in the bondcoat

Determination of the intensities

Intensity at the control volume due to the forward-moving radiation

The total intensity due to the forward-moving thermal radiation, $I_{ft}(x)$ can be expressed as

$$I_{ft}(x) = \sum_{i=1}^{N} I_f(\lambda_i, x), \quad (4)$$

where $I_f(\lambda_i,x)$ is the intensity at any point x inside the coating layer due to the forward-moving thermal radiation of wavelength, λ_i, emitted by the combustion gases. N is the total number of such wavelengths considered for calculating the total intensity. In this study, N is taken as 4 by considering four major wavelengths (0.5, 1, 3, 5 μm) that are in visible and near infrared ranges. The combustion gases emit radiations in various wavelength ranges. If the spectral intensity of combustion gases follows the Planck blackbody radiation [16], the intensity of the radiation emitted by the jth gas in the wavelength interval $\Delta\lambda_{i,j}$ about the wavelength λ_i can be written as $\varepsilon_j(\lambda_i,T_g)I(\lambda_i,T_g)\Delta\lambda_{i,j}$. Here, $\varepsilon_j(\lambda_i,T_g)$ is the emissivity of the jth gas emitting radiation at the wavelength λ_i and gas temperature T_g. $I(\lambda_i,T_g)$ is the spectral intensity of the Planck blackbody radiation [16], which is expressed in terms of the amount of energy emitted per unit area of a hot surface of temperature T_g per unit time per unit wavelength interval $\Delta\lambda_i$ about the wavelength λ_i, i.e., in units of W/cm^2 μm. The gaseous emissions may be considered isotropic and, in that case, one-half of the emitted radiation is incident on the free surface ($x = 0$) of the YSZ coating. Therefore, the total intensity of the thermal radiation of wavelength λ_i emitted by all of the combustion gases, $I_g(\lambda_i,0)$, that enters into the coating layer at $x = 0$, is given by

$$I_g(\lambda_i, 0) = \frac{1}{2}\{1 - \rho_Y(\lambda_i, T_Y(0))\} \times \sum_{j=1}^{J} \varepsilon_j(\lambda_i, T_g) I(\lambda_{i,j}, T_g)\Delta\lambda_{i,j}, \quad (5)$$

where $\rho_Y(\lambda_i,T_Y(0))$ is the reflectivity of the coating at the wavelength λ_i and the coating surface temperature $T_Y(0)$, and J is the total number of combustion species emitting radiation at the wavelength λ_i.

As the intensity $I_g(\lambda_i,0)$ propagates through the coating layer, a fraction of it (f_a) may be absorbed by the coating while the rest ($f_s = 1 - f_a$) of the radiation may scatter through the medium. Considering the absorption and scattering processes to follow the Beer–Lambert law with the appropriate wavelength- and temperature-dependent absorption coefficient, $\alpha_a(\lambda_i,T_Y(x))$, and scattering coefficient, $\alpha_s(\lambda_i,T_Y(x))$, the intensity of the forward-moving thermal radiation of wavelength λ_i can be written as

$$I_f(\lambda_i, x) = I_g(\lambda_i, 0)[f_a \exp\{-\alpha_a(\lambda_i, T_Y(x))x\} + f_s \exp\{-\alpha_s(\lambda_i, T_Y(x))x\}] \quad (6)$$

Equation 6 can be substituted into Eq. 4 to determine the total intensity, $I_{ft}(x)$, due to the forward-moving thermal radiation.

Intensity at the control volume due to the backward-moving radiation

When the forward-moving thermal radiation is incident on the coating–BC interface, a fraction of this radiation is reflected back into the coating layer as shown in Fig. 2, which enters into the control volume after traveling a distance $L_Y - x$. The intensity of this backward-moving radiation is designated by I_{b1}. The radiation that enters into the BC layer propagates toward the metal–BC interface, where a fraction of the radiation is absorbed by the metal and the rest is reflected back toward the coating–BC interface. A fraction of this reflected radiation passes through the coating–BC interface and propagates toward the control volume as a backward-moving radiation, and the rest of the radiation is reflected back toward the metal–BC interface. The metal–BC interface, in turn, absorbs a fraction of the radiation and reflects the rest toward the coating–BC interface. Thus, multiple reflections occur at these two interfaces and the coating–BC interface creates a set of backward-moving radiation field of intensities $I_{b2,1}, I_{b2,2}, I_{b2,3}, \ldots, I_{b2,U}$ due to the 1st, 2nd, 3rd,… ,Uth reflection, respectively, where U is the total number of reflections considered to account for the effect of multiple reflections. So, the total intensity at the control volume due to these two types of backward-moving thermal radiation is

$$I_{bt}(\lambda, T_Y(L_Y)) = \sum_{i=1}^{N}\left[I_{b1}(\lambda_i, T_Y(L_Y)) + \sum_{u=1}^{U} I_{b2,u}(\lambda_i, T_Y(L_Y))\right] \quad (7)$$

The expression for I_{b1} is

$$I_{b1}(\lambda_i, T_Y(x)) = I_{g0}(\lambda_i, T_Y(x))\rho_Y(\lambda_i, T_Y(L_Y)) \times [f_a \exp\{-\alpha_a(\lambda_i, T_Y(x))(L_Y - x)\} + f_s \exp\{-\alpha_s(\lambda_i, T_Y(x))(L_Y - x)\}], \quad (8)$$

where I_{g0} is the intensity of thermal radiation at the coating–BC interface, which is given by $I_{g0}(\lambda_i, T_Y(L_Y)) = I_g(\lambda_i, 0)[f_a \exp\{-\alpha_a(\lambda_i, T_Y(L_Y))\} + f_s \exp\{-\alpha_s(\lambda_i, T_Y(L_Y))\}]$. $\rho_Y(\lambda_i, T_Y(L_Y))$ is the reflectivity of the coating layer for wavelength λ_i at the temperature $T_Y(L_Y)$.

The total intensity at the control volume due to the backward-moving radiation after U reflections at the coating–BC interface can be obtained by determining the backward-moving radiation after uth reflection at this interface and summing it over all values of u ranging from 1 to U, which yields

$$\sum_{u=1}^{U} I_{b2,u}(\lambda_i, T_Y(x)) = I_{g0}(\lambda_i, T_Y(L_Y))[f_a \exp\{-\alpha_a(\lambda_i, T_Y(x))(L_Y - x)\} + f_s \exp\{-\alpha_s(\lambda_i, T_Y(x))(L_Y - x)\}] \times \{1 - \rho_Y(\lambda_i, T_Y(L_Y))\}^2 \rho_m(\lambda_i, T_m(L_m)) \times \sum_{u=1}^{U} \rho_Y^{u-1}(\lambda_i, T_Y(L_Y))\rho_m^{u-1}(\lambda_i, T_m(L_m)), \quad (9)$$

where $\rho_m(\lambda_i, T_m(L_m))$ is the reflectivity of the metal blade layer for wavelength λ_i at the temperature $T_m(L_m)$. Equation 9 is obtained by neglecting the absorption and scattering in the BC layer because its thickness is very small compared to the coating layer thickness. U is generally very large, i.e., $U \to \infty$, since a large number of multiple reflection occurs in the BC layer until the intensity of the radiation diminishes to zero within the BC layer. So, the summation factor $\sum_{u=1}^{U} \rho_Y^{u-1}(\lambda_i, T_Y(L_Y))\rho_m^{u-1}(\lambda_i, T_m(L_m))$ in Eq. 9 represents a geometric series of infinite terms. The common ratio, $\rho_Y(\lambda_i, T_Y(L_Y))\rho_m(\lambda_i, T_m(L_m))$, of this series is less than 1 since the reflectivity is less than 1 for partially reflecting surfaces. The sum of this series, therefore, can be written as $1/(1 - \rho_Y(\lambda_i, T_Y(L_Y))\rho_m(\lambda_i, T_m(L_m)))$, which simplifies Eq. 9 to the following form.

$$\sum_{u=1}^{U} I_{b2,u}(\lambda_i, T_Y(x)) = I_{g0}(\lambda_i, T_Y(L_Y))[f_a \exp\{-\alpha_a(\lambda_i, T_Y(x))(L_Y - x)\} + f_s \exp\{-\alpha_s(\lambda_i, T_Y(x))(L_Y - x)\}] \times \frac{\{1 - \rho_Y(\lambda_i, T_Y(L_Y))\}^2 \rho_m(\lambda_i, T_m(L_m))}{1 - \rho_Y(\lambda_i, T_Y(L_Y))\rho_m(\lambda_i, T_m(L_m))} \quad (10)$$

Equations 8 and 10 can be substituted into Eq. 7 to determine the total intensity, $I_b(\lambda, T_Y(L_Y))$, due to the backward-moving thermal radiation.

Intensity at the metal–BC interface due to multiple reflections in the BC layer

The multiple reflections in the BC layer generate a backward-moving radiation field as discussed above, and a forward-moving radiation field that imposes a heat flux on the metal blade at the metal–BC interface, i.e., at $x = L_m$. The total absorbed intensity of this radiation at this interface, i.e., the amount of radiative heat absorbed by the metal blade per unit surface area per unit time at $x = L_m$, due to U reflections is given by

$$I_A(\lambda_i, T_m(L_m)) = I_{g0}(\lambda_i, T_m(L_m))(1-\rho_Y(\lambda_i, T_Y(L_Y))) \times (1-\rho_m(\lambda_i, T_m(L_m)))\sum_{u=1}^{U}\rho_Y^{u-1}(\lambda_i, T_Y(L_Y)) \times \rho_m^{u-1}(\lambda_i, T_m(L_m)) \quad (11)$$

which is obtained by neglecting the absorption and scattering in the BC layer as in the case of calculating the intensity of backward-moving radiation field. As in the case of Eq. 9, the summation factor in Eq. 11 can be written as $1/(1-\rho_Y(\lambda_i, T_Y(L_Y))\rho_m(\lambda_i, T_m(L_m)))$ which simplifies Eq. 11 to the following form.

$$I_A(\lambda_i, T_m(L_m)) = I_{g0}(\lambda_i, T_m(L_m)) \times \frac{(1-\rho_Y(\lambda_i, T_Y(L_Y)))(1-\rho_m(\lambda_i, T_m(L_m)))}{1-\rho_Y(\lambda_i, T_Y(L_Y))\rho_m(\lambda_i, T_m(L_m))} \quad (12)$$

Equation 12 will be used for the heat flux boundary condition at the metal–BC interface.

Boundary conditions for governing Eqs. 2 and 3

The convection boundary condition is applied at the surface of the coating layer facing the combustion gas, which yields

$$k_Y(T_Y)\frac{\partial T_Y(x)}{\partial x} = h_g\left[T_Y(0) - T_{\infty,g}\right] \quad \text{at } x = 0, \quad (13)$$

where $T_{\infty,g}$ is the temperature of the gas far away from the coating surface $x = 0$. We apply the continuity of temperatures and heat fluxes at the metal–BC interface, i.e.,

$$T_Y(L_Y) = T_m(L_Y) \quad \text{at } x = L_Y, \quad (14)$$

which is obtained by assuming negligible temperature variation within the BC layer because it is very thin implying $L_Y \approx L_m$ and, therefore, $T_m(L_Y) \approx T_m(L_m)$, and

$$-k_Y(T_Y)\frac{\partial T_Y(x)}{\partial x} + \sum_{i=1}^{N} I_A(\lambda_i, T_m(L_m)) = -k_m(T_m)\frac{\partial T_m(x)}{\partial x} \quad \text{at } x = L_Y. \quad (15)$$

We apply the convection boundary condition at the metal–coolant interface, i.e.,

$$-k_m(T_m)\frac{\partial T_m(x)}{\partial x} = h_c\left[T_m(L_c) - T_{\infty,c}\right] \quad \text{at } x = L_c, \quad (16)$$

where h_c is the heat transfer coefficient at the coolant–metal interface, i.e., at $x = L_c$, and $T_{\infty,c}$ is the coolant temperature far away from the coolant–metal interface.

These boundary conditions will be utilized to determine the temperature distributions in the coating layer and the metal blade based on Eqs. 2 and 3.

Solutions of the governing Eqs. 2 and 3

Equations 2 and 3 are nonlinear because the thermal conductivities, $k_Y(T_Y(x))$ and $k_m(T_m(x))$, the absorption and scattering coefficients, $\alpha_a(\lambda_i,T_Y(x))$ and $\alpha_s(\lambda_i,T_Y(x))$, respectively, and the reflectivities, $\rho_Y(\lambda_i,T_Y(x))$ and $\rho_m(\lambda_i,T_m(x))$, depend on temperatures. Also these two equations are coupled through the boundary conditions. Therefore, these two nonlinear, coupled, ordinary differential equations are difficult to solve analytically. To obtain analytic solutions, these properties are evaluated at average temperatures based on the operating temperatures of the turbine system; for example, the thermal conductivity and the absorption and scattering coefficients of the coating layer are evaluated at the average value of the coating surface temperature and the coating–metal interface temperature. The reflectivity of the coating surface is evaluated at the average value of the coating surface temperature and the combustion gas temperature. The reflectivity of the metal blade at the metal–BC interface and the thermal conductivity, $k_m(T_m(x))$, are evaluated at the average value of the blade temperature at this interface and the blade temperature at the metal–coolant interface. Based on these simplifications in evaluating the material properties, the solutions of Eqs. 2 and 3 can be written as

$$T_Y(x) = \frac{1}{k_Y}F_f(x) - \frac{1}{k_Y}F_b(x) + C_1x + C_2 \quad (17)$$

and

$$T_m(x) = C_3x + C_4 \quad (18)$$

where $F_f(x)$ and $F_b(x)$ are two indefinite integrals given by $F_f(x) = \int I_{ft}(x)dx$ and $F_b(x) = \int I_{bt}(x)dx$, and C_1, C_2, C_3, and C_4 are the constants of integrations. These constants are determined by substituting Eqs. 17 and 18 in the boundary conditions (Eqs. 13–16), which yields the following expressions.

$$C_1 = \frac{g(x)}{\left[L_Y + \frac{k_Y}{h_g} - L_Y\frac{k_Y}{k_m} + \left(\frac{(k_m+h_cL_c)}{h_c}\right)\left(\frac{k_Y}{k_m}\right)\right]} \quad (19)$$

$$C_2 = \frac{k_Y}{h_g}\left[\frac{g(x)}{\left\{L_Y + \frac{k_Y}{h_g} - L_Y\frac{k_Y}{k_m} + \left(\frac{(k_m+h_cL_c)}{h_c}\right)\left(\frac{k_Y}{k_m}\right)\right\}}\right] - \frac{1}{k_Y}F_f(0) + \frac{1}{k_Y}F_b(0) + T_{\infty,g} + \frac{I_{ft}(\lambda_i, T_Y(0))}{h_g} - \frac{I_{bt}(\lambda_i, T_Y(0))}{h_g} \quad (20)$$

$$C_3 = \frac{k_Y}{k_m}\left[\frac{g(x)}{\left\{L_Y + \frac{k_Y}{h_g} - L_Y\frac{k_Y}{k_m} + \left(\frac{(k_m+h_cL_c)}{h_c}\right)\left(\frac{k_Y}{k_m}\right)\right\}}\right] + \frac{I_{ft}(\lambda_i, T_Y(L_Y))}{k_m} - \frac{I_{bt}(\lambda_i, T_Y(L_Y))}{k_m} - \frac{1}{k_m}\sum_{i=1}^{N} I_A(\lambda_i, T_Y(L_Y)) \quad (21)$$

and

$$C_4 = -\left[\frac{k_Y}{k_m}\left\{\frac{g(x)}{\left\{L_Y + \frac{k_Y}{h_g} - L_Y\frac{k_Y}{k_m} + \left(\frac{(k_m+h_cL_c)}{h_c}\right)\left(\frac{k_Y}{k_m}\right)\right\}}\right\} + \frac{I_{ft}(\lambda_i, T_Y(L_Y))}{k_m} - \frac{I_{bt}(\lambda_i, T_Y(L_Y))}{k_m} - \frac{1}{k_m}\sum_{i=1}^{N} I_A(\lambda_i, T_Y(L_Y))\right]\frac{(k_m + h_cL_c)}{h_c} + T_{\infty,c} \quad (22)$$

where

$$g(x) = -\frac{1}{k_Y}F_f(L_Y) + \frac{1}{k_Y}F_b(L_Y) + \frac{1}{k_Y}F_f(0) - \frac{1}{k_Y}F_b(0) - T_{\infty,g} - \frac{I_{ft}(\lambda_i, T_Y(0))}{h_g} + \frac{I_{bt}(\lambda_i, T_Y(0))}{h_g} + L_Y\left[\frac{I_{ft}(\lambda_i, T_Y(L_Y))}{k_m} - \frac{I_{bt}(\lambda_i, T_Y(L_Y))}{k_m} - \frac{1}{k_m}\sum_{i=1}^{N} I_A(\lambda_i, T_Y(L_Y))\right] - \left[\frac{(k_m + h_cL_c)}{h_c}\left\{\frac{I_{ft}(\lambda_i, T_Y(L_Y))}{k_m} - \frac{I_{bt}(\lambda_i, T_Y(L_Y))}{k_m} - \frac{1}{k_m}\sum_{i=1}^{N} I_A(\lambda_i, T_Y(L_Y))\right\} - T_{\infty,c}\right]$$

These expressions for C_1, C_2, C_3, and C_4 can be substituted into Eqs. 17 and 18 to obtain the temperature distributions in the coating layer and metal blade, respectively, as follows.

$$T_Y(x) = \frac{1}{k_Y}F_f(x) - \frac{1}{k_Y}F_b(x) + \frac{g(x)}{\left[L_Y + \frac{k_Y}{h_g} - L_Y\frac{k_Y}{k_m} + \left(\frac{(k_m+h_cL_c)}{h_c}\right)\left(\frac{k_Y}{k_m}\right)\right]}x + \frac{k_Y}{h_g}\left[\frac{g(x)}{\left\{L_Y + \frac{k_Y}{h_g} - L_Y\frac{k_Y}{k_m} + \left(\frac{(k_m+h_cL_c)}{h_c}\right)\left(\frac{k_Y}{k_m}\right)\right\}}\right] - \frac{1}{k_Y}F_f(0) + \frac{1}{k_Y}F_b(0) + T_{\infty,g} + \frac{I_{ft}(\lambda_i, T_Y(0))}{h_g} - \frac{I_{bt}(\lambda_i, T_Y(0))}{h_g} \quad (23)$$

and

$$T_m(x) = \left[\frac{k_Y}{k_m}\left\{\frac{g(x)}{\left\{L_Y + \frac{k_Y}{h_g} - L_Y\frac{k_Y}{k_m} + \left(\frac{(k_m+h_cL_c)}{h_c}\right)\left(\frac{k_Y}{k_m}\right)\right\}}\right\} + \frac{I_{ft}(\lambda_i, T_Y(L_Y))}{k_m} - \frac{I_{bt}(\lambda_i, T_Y(L_Y))}{k_m} - \frac{1}{k_m}\sum_{i=1}^{N} I_A(\lambda_i, T_Y(L_Y))\right]x - \left[\frac{k_Y}{k_m}\left\{\frac{g(x)}{\left\{L_Y + \frac{k_Y}{h_g} - L_Y\frac{k_Y}{k_m} + \left(\frac{(k_m+h_cL_c)}{h_c}\right)\left(\frac{k_Y}{k_m}\right)\right\}}\right\} + \frac{I_{ft}(\lambda_i, T_Y(L_Y))}{k_m} - \frac{I_{bt}(\lambda_i, T_Y(L_Y))}{k_m} - \frac{1}{k_m}\sum_{i=1}^{N} I_A(\lambda_i, T_Y(L_Y))\right]\frac{(k_m + h_cL_c)}{h_c} + T_{\infty,c} \quad (24)$$

Results and discussion

The temperature distribution within the ceramic coatings and the total heat flux through the TBC system are calculated for various material properties listed in Table 1.

To analyze how the reflectivity of the coating layer affects the temperature distribution in a TBC system, Fig. 3 is plotted for different values of the reflectivity. The surface temperature of the YSZ coating is reduced by about 45 K in the case of high (80%) reflectivity compared to the case low (20%) reflectivity. The difference in the temperature (ΔT_Y) at the YSZ coating surface ($x = 0$) and the coating–BC interface ($x = L_Y$) ranges from 8 to 11 K for different values of the reflectivity. The temperature drop within metal layer (ΔT_m) between the points $x = L_m$ and $x = L_c$ is 4 K which is lower than in the coating layer. It is clear that YSZ coatings of high reflectivity can reduce the temperature in the coating layer and metal blade.

Siegel and Spuckler [8] analyzed the effects of radiative heating on the temperature distributions and heat fluxes in TBCs using heat transfer coefficients $h_g = 3014$ W/m^2 K and $h_c = 3768$ W/m^2 K for the hot combustion gas and the coolant, respectively, in turbine engines for aerospace applications. These values may be reasonable for aerospace applications, but they are rather high for turbines in power plants. Their results showed a large temperature drop (e.g., 300 K) across the TBC thickness, which is, however, not due to good thermal barrier effectiveness, i.e., low thermal conductivity, of the TBC but due to the large heating and cooling effects, i.e., large values of h_g and h_c, respectively. Although the large values of h_g increase the heat flux on the TBC surface, the disadvantage of the large values of h_c is

Table 1 Parameters for the heat transfer model

Symbols (units)	Description	Values	Values at different wavelength (λ_i) (μm)				Reference
			$\lambda_1 = 0.5$	$\lambda_2 = 1$	$\lambda_3 = 3$	$\lambda_4 = 5$	
h_g (W/m^2 K)	Convection heat transfer coefficient of hot gas	250					[8]
h_c (W/m^2 K)	Convection heat transfer coefficient of cooling gas	110					[8]
$T_{\infty,g}$ (K)	Temperature of hot combustion gas	1423					
$T_{\infty,c}$ (K)	Temperature of cooling gas	800					[8]
$I_b(\lambda_i,T)$ (W/m^2)	Intensity of blackbody radiation at λ_i and T	($T = 1423$ K, $T = 800$ K)	6.285×10^6	4.837×10^9	1.745×10^{10}	5.814×10^9	
			0.909	1.84×10^6	1.224×10^9	1.074×10^9	
$I_g(\lambda_i,T)$ (W/m^2)	Intensity of hot gas radiation at λ_i and T	($I_g = \varepsilon_g I_b$) ($T = 1423$ K)	6.285×10^4	1.209×10^9	1.309×10^{10}	5.814×10^9	
$I_m(\lambda_i,T)$ (W/m^2)	Intensity of metal radiation at λ_i and T	($I_m = \varepsilon_m I_b$) ($T = 1112$ *K*)	0.864	1.656×10^6	8.568×10^8	8.055×10^8	
$\varepsilon_g(\lambda_i,T)$	Emissivity of combustion gas at λ_i and T	($T = 1423$ *K*)	0.01	0.25	0.75	1	[17]
$\varepsilon_Y(\lambda_i,T)$	Emissivity of YSZ at λ_i and T	($T = 1112$ K)	0.75	0.1	0.29 ($T = 1273$ K)	0.25 ($T = 1273$ K)	[18]
$\varepsilon_m(\lambda_i,T)$	Emissivity of metal at λ_i and T	($T = 1112$ K)	0.95	0.9	0.7 ($T = 300$ K)	0.75 ($T = 300$ K)	[18]
$\rho_Y(\lambda_i,T)$	Reflectivity of YSZ at λ_i and T	($T = 1112$ K)	0.28 ($\varepsilon = 0.75$)	0.9 ($\varepsilon = 0.1$)	0.71 ($\varepsilon = 0.29$)	0.75 ($\varepsilon = 0.25$)	[18]
$\rho_m(\lambda_i,T)$	Reflectivity of metal at λ_i and T	($T = 1112$ K)	0.05 ($\varepsilon = 0.95$)	0.1 ($\varepsilon = 0.9$)	0.3 ($\varepsilon = 0.7$)	0.25 ($\varepsilon \approx 0.75$)	[16]
$\alpha_a(\lambda_i,T)$ (m^{-1})	Absorption coefficient of YSZ layer at λ_i and T	(at 300 K)	50	30	35	400	[8]
$\alpha_s(\lambda_i,T)$ (m^{-1})	Scattering coefficient of YSZ layer at λ_i and T	(at 300 K)	23,100	15,050	10,030	9400	[8]
k_Y (W/m K)	Thermal conductivity of YSZ	3.5 (at 300 K)					0.7–3.5 [2]
k_m (W/m K)	Thermal conductivity of superalloy metal	33 (at 300 K)					[8]
L_Y (m)	Thickness of TBC layer	7.94×10^{-4}					
L_m (m)	Thickness of TBC layer and metal blade	4.24×10^{-3}					
L_c (m)	Thickness of TBC layer, BC and metal blade	5×10^{-5}					[8]

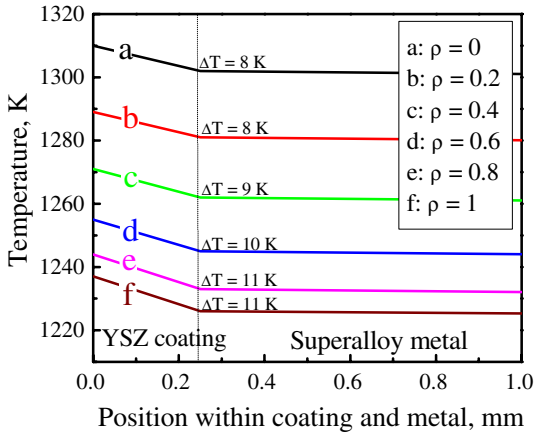

Fig. 3 Effect of the TBC reflectivity on the temperature drop across the TBC layer and the metal blade

that a large amount of thermal energy is lost to the coolant and, therefore, much of the energy of the combustion fuel is not utilized by the turbine system for power generation. Wang et al. [7] used the heat transfer coefficients $h_g = 250$ W/m^2 K for the hot combustion gas and $h_c = 110$ W/m^2 K for the coolant, which are considered reasonable for turbines in power plants, and showed relatively small temperature drop (e.g., 34 K) across the multiple-layered TBC thickness. Both studies [7, 8], however, ignored the volumetric heating due to the propagation of radiation in the TBC layer. The volumetric heating is considered in our model and the temperature drop across the TBC thickness is found to be very small (8–11 K), indicating that high-temperature gaseous radiation heats up the interior of the TBC layer and thus reduces the thermal barrier effectiveness of TBC.

The effects of the relative magnitudes of the radiation absorption and scattering are also analyzed and presented in Fig. 4 for different values of the absorption fraction (f_a) and scattering fraction (f_s), which show that the drops in temperature across both the coating layer and the metal blade are higher in the case of low absorption fraction ($f_a = 0.2$) and high scattering fraction ($f_s = 0.8$) than in the case of $f_a = 0.8$ and $f_s = 0.2$. The effect of scattering in the material is generally small when the absorption coefficient is large. The reciprocal of these coefficients can be considered as the mean distance traveled by the thermal radiation before absorption or scattering occurs. The smaller the coefficient, the larger would be the distance traveled by the thermal radiation before being absorbed or scattered. The absorption of thermal radiation is the process by which the energy of a photon is taken up by a material, typically by the electrons of an atom, and the absorbed radiant energy is transformed to the electric potential energy of the atom. Several phenomena can occur to this absorbed energy, since it may be re-emitted by the electron as scattered radiant energy, dissipated to the rest of the material as heat, or even the electron can be freed from the atom. The heated material, in turn, can emit radiation as in the case of the blackbody emission of radiation. The temperature of a material changes when it absorbs or emits thermal radiation. Absorption and emission, therefore, affect the temperature distribution in a material. Scattered thermal radiation, on the other hand, does not affect the temperature of a material unless it is absorbed. So, increasing the scattering coefficient of TBCs is a possible approach to reduce the volumetric heating of TBCs by thermal radiation. Furthermore, the heat conduction by phonons, which are the quanta of energy for various vibrational modes of a solid, can be affected by limiting the phonon mean free path. These quanta of energy, therefore, are also affected by the absorption and scattering coefficients [1, 2].

The effects of the thermal conductivity of YSZ are presented in Fig. 5. It shows that the temperature reduction

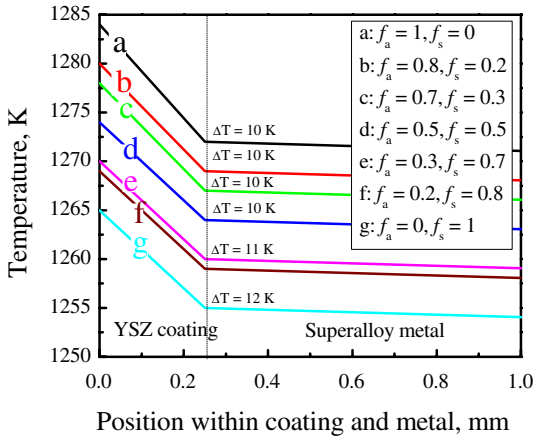

Fig. 4 Effect of the fraction factor of scattering and absorption on the temperature drop across the TBC layer and the metal blade

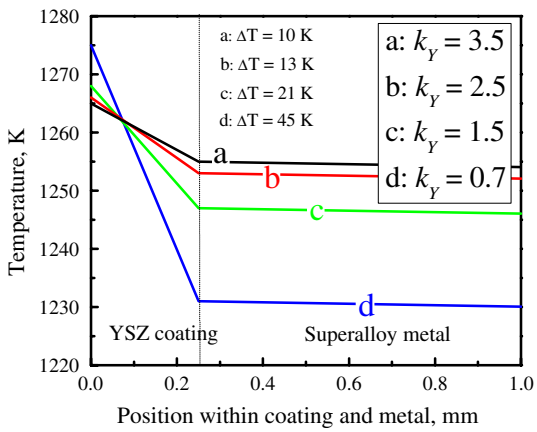

Fig. 5 Effect of the TBC thermal conductivity on the temperature drop across the TBC layer and the metal blade

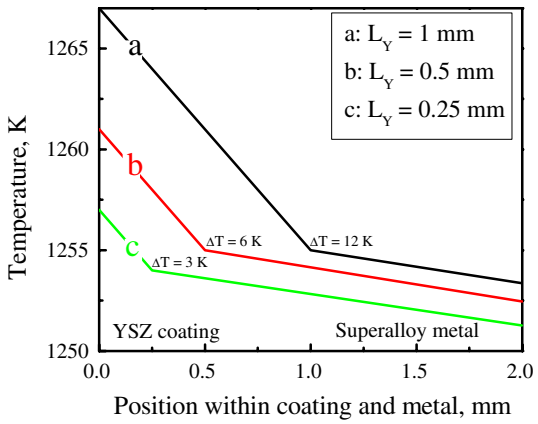

Fig. 6 Effect of the TBC thickness on the temperature drop across the TBC layer and the metal blade

in the TBC layer is more significant for low (0.7 W/m K) thermal conductivity than for high (1.5, 2.5, or 3.5 W/m K) thermal conductivities. These values of thermal conductivity are based on the data used by Klemens and Gell [2]. This reduction in temperature depends on both the thermal conductivity and the volumetric heating by the thermal radiation. Since the intensity of the thermal radiation varies along the TBC thickness, the temperature drop across the TBC layer is examined in Fig. 6 for different values of the TBC thickness ranging from 0.25 to 1 mm. The thermal resistance of a material decreases as its thickness decreases. So, it is expected that the surface temperature of the coating and the temperature drop across it will decrease as the coating thickness decreases. In crystalline solids, heat is transferred by three mechanisms: free electrons, lattice vibrations, and radiation [19]. Since YSZ is an electrical insulator, free electrons are not expected to contribute to the total thermal conductivity of YSZ. So, the lattice vibrations (phonons) and the radiations (photons) will affect the flow of thermal energy within the TBC layer. The contribution of lattice vibration to the thermal conductivity of YSZ can be expressed by $k_Y = 1/3 \int C_V \rho \bar{v} l_p$, where C_V is the specific heat capacity at constant volume, ρ is the density, $\bar{v}$ the phonon velocity, and l_p is the mean free path of phonons [6, 19]. Any of these four parameters can be reduced to decrease the thermal conductivity. Since large thicknesses of the coating increase its thermal resistance, a large temperature drop can be achieved across the TBC layer for thick coatings. However, thick coatings offer longer distances for the propagation and absorption of radiation causing radiative heating over a large volume of the coating. So, a thick coating has two opposite effects. While it increases the temperature drop across the TBC layer owing to conduction heat transfer, it simultaneously decreases the temperature drop owing to volumetric heating by thermal radiation. However, the radiative heating can be reduced by designing a coating of high reflectivity at all the wavelengths of the radiation emitted by the combustion gas. It should be noted that low thermal conductivity also increases the thermal resistance of a material. So, a coating of large thickness, low thermal conductivity, and high reflectivity will be an effective TBC for both conductive and radiative heating. Rare earth oxides such as CeO_2, HfO_2, Y_2O_3, and Sc_2O_3, or other oxides such as In_2O_3 and Al_2O_3 can be incorporated into the TBC material to increase its reflectivity at high temperatures. These oxides need to be used in small amounts so that they do not change the metallurgical composition of the TBC significantly. Such additives will, therefore, enable improving the radiative properties of the coating while maintaining the oxidation- and corrosion-resistant properties of current TBC in harsh environments.

For quantitative analysis of the TBC design parameters, such as the TBC thickness, thermal conductivity, and reflectivity, the temperature drop (ΔT) across the TBC layer is generally considered a critical parameter because ΔT increases as the TBC thickness increases and its thermal conductivity decreases. This trend is shown in Fig. 7a. Low thermal conductivity ($k_Y = 0.7$) and thick (1 mm) coating of TBC have a large temperature drop ($\Delta T = 113.48$ K) between $x = 0$ and $x = L_Y$, i.e., across the TBC layer.

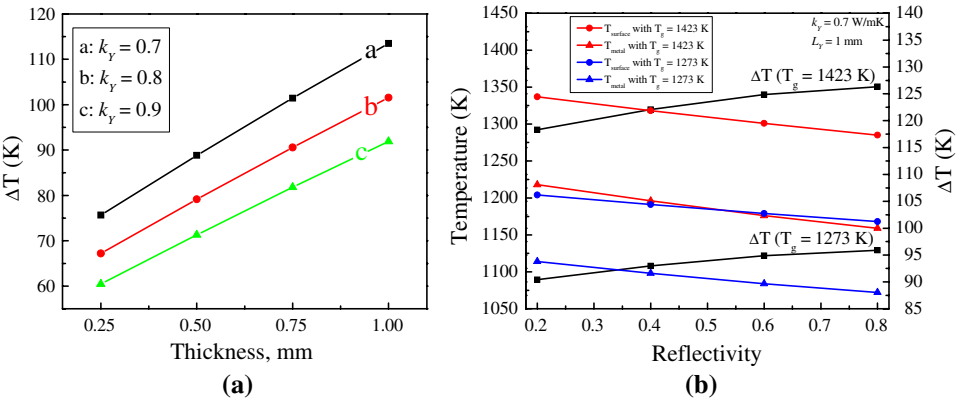

Fig. 7 **a** Effect of the TBC thickness on the temperature drop (ΔT) across the TBC layer for different thermal conductivities. **b** Effect of reflectivity of the temperature drop (ΔT) and TBC surface temperature ($T_Y(0)$) and the TBC–metal blade interface temperature ($T_Y(L_Y)$ and $T_m(L_Y)$) for different combustion gas temperatures (T_g = 1423 and 1273 K). k_Y = 0.7 W/mK, L_Y = 1 mm, f_a = 0.6 and f_s = 0.4

However, ΔT alone is not a critical parameter to understand the effect of radiative heating because the radiation can heat up both the TBC surface and the metal blade, which may reduce the value of ΔT but heat up the metal blade above its safe operating temperature. Therefore, Fig. 7b is plotted to show ΔT and the TBC surface and metal blade temperatures as a function of reflectivity, where $k_Y = 0.7$ and $L_Y = 1$ mm have been chosen as the typical values for TBC. Two sets of results are plotted, one for the combustion gas temperature $T_g = 1423$ K and the other for $T_g = 1273$ K, to show that highly reflective TBC allows operating a typical turbine system at higher combustion gas temperatures without increasing the value of ΔT significantly. The TBC surface and the metal blade temperatures decrease as the reflectivity increases. Therefore, high reflectivity such as $\rho = 0.8$, which yields high temperature drop ($\Delta T = 126.34$ K) and low TBC surface and metal blade temperatures ($T_Y(0) = 1285$ K and $T_Y(L_Y) = 1159$ K) for the combustion gas temperature $T_g = 1423$ K, would be a desirable property for TBC to act as RBC.

Conclusions

Conduction and radiative heatings are two heating modes for TBC. Only the conduction mode is generally considered for TBC design. The radiative heating is important at high combustion temperatures. A one-dimensional heat transfer model, which includes the effect of radiative heating, is developed for the temperature distributions in the coating layer and the metal blade beneath the coating. The volumetric heat source caused by the absorption of radiation decreases the temperature drop across the TBC layer significantly. A radiation barrier coating is necessary to mitigate this effect and such coatings can be designed by increasing the reflectivity, scattering coefficient, and coating thickness, and by decreasing the absorption coefficient and thermal conductivity. Increased thickness, low conductivity, and high reflectivity of TBC increase the operating temperature of turbine engines.

Acknowledgement This work was supported by the Siemens Westinghouse University Embryonic Technology Program, 2007, which was managed by Robert E. Shannon, Manager, Siemens Advanced Technology Development and Emerging Technologies Department.

References

1. Klemens PG (1993) Thermochim Acta 28:247
2. Klemens PG, Gell M (1998) Mater Sci Eng A 245:143
3. Singh J, Wolfe DE (2005) J Mater Sci 40:1. doi:10.1007/s10853-005-5682-5
4. Trice RW, Jennifer Su Y, Mawdsley JR, Faber KT, De Arellano-Lopez AR, Wang H, Porter WD (2002) J Mater Sci 37:2359. doi:10.1023/A:1015310509520
5. Eldridge JI, Spuckler CM, Street KW, Markham JR (2002) Ceram Eng Sci Proc 23:417
6. Kelly MJ, Wolfe DE, Singh J, Eldridge JI, Zhu DM, Miller R (2006) Int J Appl Ceram Technol 3:81
7. Wang D, Huang X, Patnaik P (2006) J Mater Sci 41:6245. doi:10.1007/s10853-006-0494-9
8. Siegel R, Spuckler CM (1998) Mater Sci Eng A 245:150
9. Viskanta R, Kim DM (1980) J Heat Transf 102:182
10. Mahapatra SK, Nanda P, Sarkar A (2005) Heat Mass Transf 41:890
11. Spuckler CM, Siegel R (1994) J Thermophys Heat Transf 8(2):193
12. Bennet TD (2003) Int J Heat Mass Transf 46:2341
13. Sadooghi P (2005) J Quant Spectrosc Radiat Transf 92:403
14. Wellele O, Orlande HRB, Ruperti JN, Colaco MJ, Delmas A (2006) J Phys Chem Solids 67:2230
15. Demange D, Bejet M (2004) Aerosp Sci Technol 8:321
16. Siegel R, Howell JR (1992) Thermal radiation heat transfer, 3rd edn. Taylor & Francis, New York
17. Viskanta R, Menguc MP (1987) Prog Energy Combust Sci 13:97
18. Eldridge JI, Spuckler CM, Martin RE (2006) Int J Ceram Technol 3(2):94
19. Kingery WD (1976) Introduction to ceramics, 1st edn. Wiley, New York